Accident Analysis and Prevention 133 (2019) 105298

Contents lists available at ScienceDirect

Accident Analysis and Prevention

journal homepage: www.elsevier.com/locate/aap

Structural equations modeling of real-time crash risk variation in car-following incorporating visual perceptual, vehicular, and roadway factors

Naikan Ding (Ph.D)[a,*], Nisha Jiao[b], Shunying Zhu (Ph.D)[c], Bing Liu (Ph.D)[c]

[a] 206 Guanggu 1st Road, School of Civil Engineering and Architecture, Wuhan Institute of Technology, Wuhan, 430205, China
[b] 428 Jianshe Avenue, Planning Research Studio, Department of Transportation of Hubei Province, Wuhan, 430030, China
[c] 1178 Heping Avenue, School of Transportation, Wuhan University of Technology, Wuhan 430063, China

ARTICLE INFO

Keywords:
Real-time crash risk variation
Car-following
Horizontal curves
Line markings
Structural equations modeling

ABSTRACT

In this study, we attempted to explain drivers' crash risk variation in car-following for crash avoidance considering the effects of drivers' visual perception, vehicle type, and horizontal curves, with a structural equations model. The model was built by incorporating drivers' speed risk perception and distance risk perception as latent variables. A series of on-road experiments was conducted on the curved segments of a freeway in China to collect naturalistic driving data to approximate the model. The results indicate that (1) the amount of variance in speed risk perception accounted for by the temporal and spatial frequency and the following vehicle type was 21%; (2) the amount of variance in distance risk perception accounted for by the temporal and spatial frequency, leading vehicle type, stopping sight distance (SSD), horizontal sightline offset (HSO), and radius was 29%; and (3) speed risk perception and distance risk perception explained 27% of the total variance in crash risk variation, which is significantly higher than previous similar results that were commonly limited to 10%. The results were explained from the perspective of the effect of line markings, vehicle type (size), and curves on driving behaviors, respectively. In addition, the difference between the effect of speed risk perception and distance perception on crash risk variation was discussed considering the direct and indirect origins of risk in driving. The findings suggests that the incorporation of visual perceptual, vehicular, and roadway factors and its relevant speed risk perception and distance risk perception can better explain the crash risk in car-following. This study also emphasized the possibility and the need of applying the line markings as a visual intervention to prevent the drivers from rear-end crashes on curves, which may provide new insights and be a new solution for roadway safety.

1. Introduction

According to the World Health Organization (WHO, 2018), over 1.3 million people die each year on roads, making road traffic crashes a leading cause of death globally, and the leading cause of death among those aged 5–29 years. Most of these deaths are in low- and middle-income countries where rapid economic growth has been accompanied by increased motorization and road traffic injuries. In China, there were 63,772 deaths and 209,654 injuries reported in over 8.4 million road traffic crashes in 2017 (Traffic Management Bureau of the Public Security Ministry, 2018). Rear-end crashes are among the more common accident types, accounting for 36.5% of all reported accidents and 32.8% of all fatalities on freeways in China in 2017 (Traffic Management Bureau of the Public Security Ministry, 2018).

In light of the shocking numbers, significant efforts have been made in investigating various factors leading to rear-end crashes over the past decades. According to Highway Safety Manual (AASHTO, 2010), and to the nature of a surface transportation system, roadway crashes can be attributed to a combination of drivers (human factors), vehicles (vehicular factors), and road infrastructure (roadway factors). The human factors, like biased perception (Dewar and Olson, 2007), are the predominant factors as the vast majority of the rear-end crashes can occur if the following driver errs in judging closing speed and headway to the leading vehicle. Specifically, the drivers' visual perception are the major human factors affecting driving behaviors, because more than 90% of the information that drivers obtain and use is visual (Sivak, 1996). Accordingly, the perception of speed and distance are two critical aspects for drivers to successfully avoid a crash. Consistent to a person's perception of motion in the three-dimensional space, drivers' perception of speed and distance are also greatly environmental depended, more specifically, the road surface. The most relevant vehicular factors would be the vehicle size (type) and the composition of traffic

* Corresponding author.
E-mail addresses: nding@wit.edu.cn (N. Ding), 421946755@qq.com (N. Jiao), zhusy2001@163.com (S. Zhu), lbjiaotong@126.com (B. Liu).

https://doi.org/10.1016/j.aap.2019.105298
Received 17 June 2019; Received in revised form 9 September 2019; Accepted 12 September 2019
Available online 23 September 2019

flow or the percentage of heavy (large) vehicles (Golob et al., 2004; Nagatani, 2015), because the drivers would probably perceive a threat both in visual and in mental when there is a large vehicle in front of them. As for roadway factors, there is a great deal of road elements could be the influential to traffic safety, such as road alignment, affiliated facilities, and road pavement, etc. Among these elements, the horizontal curves (radius) and its relevant stopping sight distance (SSD) could be two of most prevalent factors related to accidents (Harwood and Bauer, 2015; Wood and Donnell, 2014; Wood and Donnell, 2017), because the curves are more likely to be a natural hazard to drivers due to the changes in driving expectancy and vehicle handling.

Though enormous research has been done to attempt to associate the crash risk and various contributing factors, there is lack of consideration of the effects of drivers' visual perception on driving behavior and crash risk. As a matter of fact, the perception of speed and distance are the original stimulus of risk of drivers to estimate the potential of crash and to successfully avoid a crash. Besides, crash risk analysis is usually conducted based on archived traffic accident data, which is probably deficient in statistical integrity and accuracy. So, in this paper, a conflict-based surrogate safety measure was used to match the real-time crash risk analysis with naturalistic driving data. With these considerations in mind, the primary objective of this paper is to explore the association between rear-end crash risk on freeway segments and the visual perceptual, vehicular, and roadway factors that are mentioned above. The visual perceptual factors were manipulated and controlled as a certain optical flow information on road surface, while the vehicle size and the stopping sight distance were observed according to the naturalistic traffic flow and the road alignment per se. The real-time crash risk under naturalistic riving situation was measured by conflicted-based surrogate indicators, such as time-to-crash (TTC) and deceleration rate to avoid a crash (DRAC). The possible association between crash risk and the contributing factors was established by a structural equations model.

The remainder of the paper is organized as follows. Following the introduction, a review of the technical literature is presented in Section 2. Section 3 constructs a theoretical framework of structural equations model concerning the rear-end crash risk. Section 4 describes the empirical methodology and data collection, followed by the results of structural equations modeling in Section 5. A discussion of the modeling results appears in Section 6. Section 7 concludes the research findings.

2. Literature Review

2.1. Visual perceptual factors

Visual information and visual perceptual factors, to a greater extent, are cognitive psychological concepts, which can be derived from the theory of Gibson (1950), who interpreted the observers' visual perception as that there was continuous light entering and "flowing" through its retina, when the observer was seeing moving objects. And that was the so-called "optic flow". Optic flows can be produced by motions of objects with respect to the background or by motions of the perceiver per se. Visual perceptual factors can further be categorized into speed perceptual factors and distance perceptual factors that correspond to the two basic parameters in traffic flow. Edge rate (ER) is one of optical variables, relates greatly to the speed perception of observers. It was defined as the rate at which local discontinuities cross a fixed point of reference in the observer's field of view Warren (1982), and it is essentially related with the temporal frequency (measured by the unit of Hz) and spatial frequency produced by the relative motion between the discontinuous elements and the drivers. Though edge rate is not common seen in transportation research domain, it has been widely and unconsciously used in speed reduction countermeasures, e.g., the converging chevron marking pattern (Drakopoulos and Vergou, 2003) and the transverse markings (Gates et al., 2008; Martindale and Urlich, 2010), which may create an illusion of travelling faster. In addition, some empirical studies, with field observations, have verified that the longitudinal line markings (Liu et al., 2013; Zhao et al., 2018) or transvers line markings (Denton, 1980; Retting et al., 2000; Rakha et al., 2006) on road surface could lead to an effect of speed reduction, if the markings were spacedly and regularly installed with a certain gap. Also, the psychological mechanisms responsible for speed reductions caused by the line markings were also investigated using virtual-reality (Francois et al., 2011), driving simulator (Godley et al., 2000), and on-road experiments (Liu et al., 2013), which all argued that edge rate could cause overestimation in self-speed of drivers, which in turn led to speed reductions. In particular, (Liu et al., 2013) found that the drivers almost unanimously decelerated when the edge rate ranged from 8 Hz to 16 Hz.

Optic flow also matters in drivers' distance perception. According to Gibson's "Ground Theory" (Gibson, 1950), the visual system was unable to establish a reliable reference frame with result of failure to obtain correct absolute distance, when the common ground surface disrupted (discontinued). Based on the fundamental "Ground Theory", Sinai et al. (1998), Yarbrough et al. (2002), and Wu et al. (2004) verified that the "discontinuous" ground surface visual information was able to lead to a phenomenon of distance underestimation among observers, which was also referred to as the "discontinuity effect" by (Feria et al. (2003)). By absorbing the results and thoughts from the above research, Ding et al. (2017a), Ding et al. (2017b), Ding et al. (2019) conducted a series of on-road experiments with longitudinal or transverse line markings installed on road surface of freeways to visually intervene drivers' car-following behavior, and the field observations revealed that the car-following time headways were increased after the installation of the line markings. Fig. 1 explains the edge rate (ER) and relevant important terms appeared in this study.

2.2. Vehicle type

Different types of vehicles hold different car-following behaviors (Peeta et al., 2005), this difference could be a reason for rear-end crashes. Research have shown that different types (sizes) of vehicles exhibited differences in distance and time headway when following or being followed. Yoo and Green (Yoo and Green, 1999) studied the following characteristics of small passenger cars, large trucks, and buses through driving simulation tests, and found that the distance between the subjects and the small passenger cars was 10% smaller than that of other models. By naturalistic driving study, Jiang et al. (2011) reported similar results withYoo and Green (Yoo and Green, 1999), and Jiang explained that the large vehicles looked "big" in appearance, making the following drivers more cautious, which led to a greater time headway. From the perspective of visual perception, Yilmaz and Warren, 1995 and Andersen et al. (1999) attributed this "big" appearance to the reciprocal of the expansion rate of the visual angle between the following driver and its leading vehicle, which was originally marked as "τ" by Lee (1976).

2.3. Horizontal curves

Curved segments are naturally the accident-prone locations on roadways, or rather those segments with small radiuses (large curvatures) on freeways. Zegeer et al. (1991), (Schneider et al. (2009), Schneider et al. (2010), and Khan et al. (2012) discovered that the radius and degree of curvature were significant variables influencing crashes on horizontal curves, and the crash rates increased as the degree of curvature increased. For this issue, one of the prevalent arguments is that, the detection of crash events on curved trajectories is more difficult than the detection on straight trajectories (Ni and Andersen, 2008; Zhang et al., 2013; Bian et al., 2013). Ni and Andersen, (2008) believed that the information of rate of bearing change was used by observers to detect the impending crashes on curved trajectories.

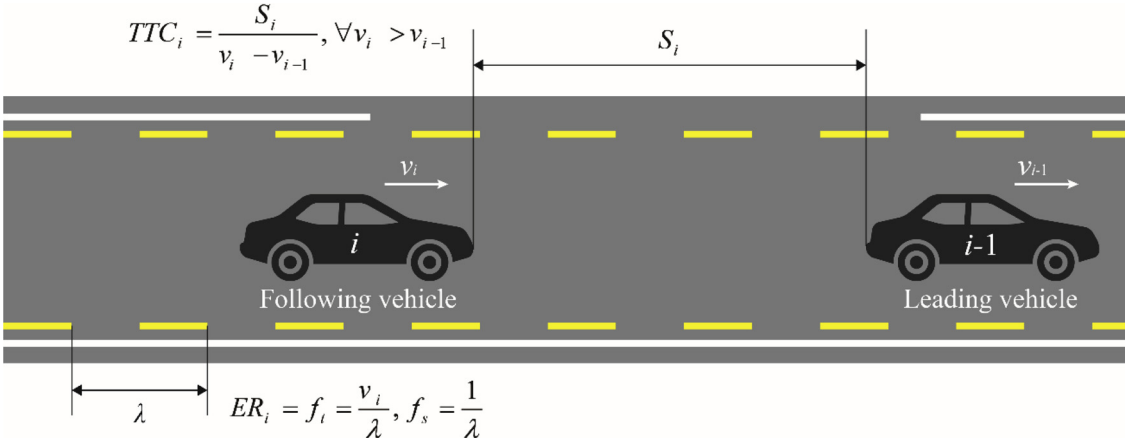

Fig. 1. An introductory sketch of the line markings and important terms. Wherein v_i, v_{i-1} are the speed of the following (i) and leading ($i-1$) vehicle on the same lane, m/s; S_i is the spacing between the two vehicles, m; TTC_i is the time-to-crash of the following vehicle (i), s; λ is one unit of the line markings series, m; f_t (or ER_i) is the temporal frequency of the line markings flashing through as the following vehicle (i) passes by at the speed of v_i, Hz; f_s is the spatial frequency of the line markings, which is only related to the spatial layout of the line markings and independent of the vehicle speed.

The role of rate of bearing change was approved by Zhang et al. (2013) and Bian et al. (2013), and the latter also thought that on straight segments, the objects were static in the visual field of observers, but on curved ones, they kept moving. Besides, according to a recent study of Llopis-Castelló et al. (2019), the effects of horizontal curves on crashes could also be attributed to the poor level of the road geometric consistency, which can be defined as how drivers' expectancies and road behavior fit. It means that the drivers' expectancies were less likely achieved on curves than on a straight one, which eventually leads to an increased likelihood of crash occurrence on curves, and especially the one with small radiuses.

Stopping sight distance (SSD) was another critical element concerning safety at horizontal curves. The minimum SSD is the distance required for a driver to successfully stop when a hazard or obstruction is on its course on a roadway. In order to ensure safe and efficient operation, the roadway must be designed with an available sight distance that exceeds the minimum SSD. The minimum SSD is a function of design speed, driver perception-reaction times, and driver deceleration rates (Fambro et al., 1997; AASHTO. A policy on geometric design of highways and streets, 2011). Besides, the horizontal sightline offset (HSO), associated with SSD, is the most important indicator for evaluating the lateral clearance on the inside of horizontal curves, which is also an indispensable roadway alignment parameter associated with traffic safety. Wood and Donnell (2014), Wood and Donnell (2017), (Himes and Donnell (2014), and Gargoum et al. (2018) argued that the SSD and HSO were vital important factors on horizontal curves to avoid crashes.

2.4. Real-time crash risk analysis

In order to evaluate the real-time crash risk, some surrogate safety measures have been used to associate the risk and traffic operating variables (Abdel-Aty et al., 2005; Xu et al., 2013; Li et al., 2014; Li et al., 2017; Mahmud et al., 2017). As comprehensively reviewed by Mahmud et al. (2017), the surrogate safety indicators were categorized into time, distance, and deceleration based conflict indicators. The most fundamental temporal indicator would be time-to-crash (TTC), and many other TTC based and/or alike temporal indicators, such as exposed time to crash (TET), time integrated TTC (TIT), and post-encroachment time (PET), etc., are also frequently used in practice to evaluate the propensity of a crash. Also, the traffic conflict can be approximated by distance based indicators, like proportion of stopping distance (PSD), margin to crash (MTC), and difference of space distance and stopping distance (DSS). Besides, dangerous situations are normally defined using the rate deceleration during emergency, so deceleration based crash risk indicators are also of great importance to evaluate the potential crash occurrence. Among them, the deceleration rate to avoid a crash (DRAC) is one of the most important and most studied indicators, which considers the role of speed differentials and deceleration of vehicles.

One of the methods for estimating the interactive causality between the various factors and their corresponding latent variables is using structural equations (Washington et al., 2010). Structural equations modeling (SEM) allows a simultaneous estimation of several equations of independent and dependent variables, thus allowing a multi-layered model to be assessed. SEM is a technique that can handle a large number of endogenous and exogenous observed variables simultaneously.

In this study, a complex experimental design was constructed to capture several aspects of factors influencing drivers' crash risk in car-following - visual perceptual, vehicular, and roadway factors. This was achieved by a series of on-road experiments conducted on three curved segments of a freeway in China, and with evidence from naturalistic driving data.

3. Theoretical Framework

Essentially, car-following is a state that the crash risk continuously exists and evolves while the drivers perceive various stimuli from its leading vehicle and environment. Yet, the primitive stimuli to formulate a crash risk in drivers are nothing more than the risk perception induced by variations on speed and/or distance. Because an increasing self-speed and/or a decreasing relative distance to the leading vehicle would generate substantial threats to the following drivers. The risk perception from speed and distance are naturally corresponded with the drivers' speed perception and distance perception, which are greatly environmental depended as explained above. Therefore, combined with the analyses in the Introduction and Literature Review, here in this study, the radius, SSD, and HSO of horizontal curves, the type of the leading and following vehicle, f_t, and f_s were set as observed variables, drivers' risk perception from speed and distance (i.e., speed risk perception and distance risk perception) were set as the exogenous latent variables, and real-time crash risk variation was set as the endogenous latent variable. According to the Green Book (AASHTO. A policy on geometric design of highways and streets, 2011), the SSD and HSO are depicted as follows.

Then, according to the geometric relationship depicted in Fig. 2, the SSD and HSO can be calculated as follows respectively:

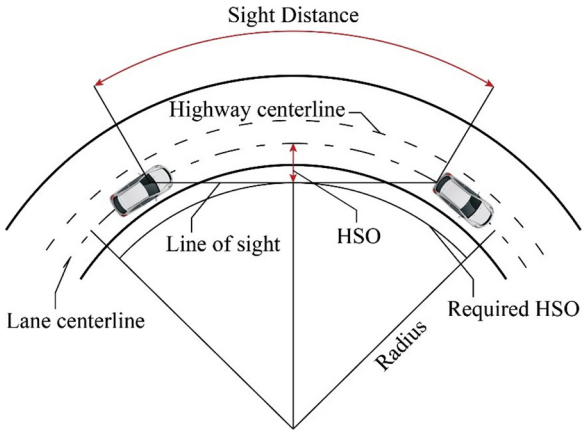

Fig. 2. Stopping sight distance and horizontal sight offsets.

$$\mathrm{SSD}=\frac{V^2}{2g\left(\left(\frac{a}{g}\right)+G\right)}+V\bullet t_r \tag{1}$$

where V is the velocity of vehicle, m/s; $g = 9.8\ \mathrm{m/s^2}$;a is the deceleration rate, $\mathrm{m/s^2}$; G is the average grade; and t_r is drivers' reaction time, s.

$$HSO = R\left[1-\cos\left(\frac{28.65\times SSD}{R}\right)\right] \tag{2}$$

where R is the radius of circular part of curve, m.

As introduced above, appropriate visual information would lead to possible speed reduction and/or distance underestimation. In this regard, here we chose TTC and DRAC to synthetically characterize the real-time crash risk with considerations of the effects of visual information on speed and distance. Wherein, TTC can be calculated according to the formula presented in Fig. 1. Further, here we modified TTC as 1/TTC to attempt to approximate crash risk more directly. Then, the modified TTC, might as well be denoted as mTTC, can be calculated as follows:

$$mTTC_i(t)=\frac{v_i(t)-v_{i-1}(t)}{S_i(t)},\ \forall\ v_i(t)>v_{i-1}(t) \tag{3}$$

where $mTTC_i(t)$ is the modified TTC of following vehicle (i) at timestamp t, $v_i(t)$ and $v_{i-1}(t)$ are the velocity of following vehicle (i) and leading vehicle ($i-1$) at timestamp t, and $S_i(t)$ is the spacingbetween the two vehicles at timestamp t.

DRAC can be calculated as follows:

$$DRAC_i(t)=\begin{cases}\dfrac{[v_i(t)-v_{i-1}(t)]^2}{x_{i-1}(t)-x_i(t)-L_{i-1}}, & v_i(t)>v_{i-1}(t)\\ 0, & v_i(t)<v_{i-1}(t)\end{cases} \tag{4}$$

where $DRAC_i(t)$, $x_i(t)$, and $v_i(t)$ are the DRAC, position, and velocity of following vehicle (i) at timestamp t, and L_{i-1} is the length of leading vehicle ($i-1$).

Yet, for the purpose of measuring the variation of crash risk during a period of time or a range of distance, we introduced two extended indicators based on $mTTC_i(t)$ and $DRAC_i(t)$, respectively. That was, the rate of change of $mTTC_i(t)$, as follows:

$$r_{mTTC}=\frac{mTTC_i(t)-mTTC_i(t+\Delta t)}{mTTC_i(t)} \tag{5}$$

and the rate of change of $DRAC_i(t)$, as follows:

$$r_{DRAC}=\frac{DRAC_i(t)-DRAC_i(t+\Delta t)}{DRAC_i(t)} \tag{6}$$

where r_{mTTC}, r_{DRAC} are the rate of change of mTTC and DRAC of vehicle i during a period of Δt after the timestamp t, respectively.

The observed and latent variables are shown in Table 1, and their theoretical relationship is depicted in Fig. 3.

4. Methodology

4.1. Experimental site

Three curved segments of the Shanghai and Chongqing Freeway (coded G50) at Yichang, Hubei Province, China, were chosen as the experimental sites (see Fig. 4). An overview and a detailed description of the segments were shown in Fig. 4 and Table 2, respectively. Note that there was no tunnel or overpass within 300 m area, nor any exposed surveillance device for violation capture.

4.2. Experimental design

A series of pre-formed adhesive yellow tapes was placed just inside both edges of the slow lane of the curved segments to exhibit line markings (see Fig. 5). And a 300 m-length slow lane was installed with this line markings. As described in our previous study (Ding et al., 2017a; Ding et al., 2017b), the speed varied from 50 km/h to100km/h, three units of the line markings were adopted, i.e., $\lambda = 2$ m, $\lambda = 4$ m, and $\lambda = 8$ m. Then, according to the mathematical relationship introduced in Fig. 1, the corresponding f_s were 0.5, 0.25, and 0.125 respectively, and f_t ranged from 1.7 Hz to 13.9 Hz. Fig. 5 demonstrates the design and layout of the line markings with $\lambda = 2$ m on curve3 (R = 800 m) as an example.

4.3. Data collection and treatment

4.3.1. Data collection

In general, considering the relative position of a driver in the vehicle to the inner side of the curved segment, we collected the traffic flow data of the two opposite directions of each curved segment at the same time to minimize the possible impact from turning direction of the curve. The traffic flow data were collected by using NC200 traffic analyzers and cameras. Yet, due to an insufficient number of traffic analyzers and cameras, the data collection process can only be carried out on one segment at a time. In specific, we adopted similar methods as in our previous experiments (Ding et al., 2017a) to collect traffic flow data. That was, for one direction of a curved segment, we sequentially positioned three NC200 traffic analyzers in the center of the slow lane of a segment, which represented three observation sections, to collect speed, distance, time headway, and vehicle type at each observation section (see Fig. 6). To accurately extract out the data of the same vehicle at each section from the traffic analyzers, the system time of traffic analyzers were synchronized with the Beijing standard time before every single test. Meanwhile, in case of failures on data collection of the traffic analyzers, three video cameras (50 frames of images with a resolution of 1920 × 1080 recorded per second) were used for possible data verification. If there was a significant difference between the data from the analyzers and from the cameras, re- observation would be initiated. The cameras were mounted outside the crash barrier on the hard shoulder with the same level in horizontal with regard to its corresponding traffic analyzers. To avoid being mistakenly regarded as traffic violation surveillance by drivers, the cameras were sheltered with local shrubs and invisible from the lanes. For the opposite direction of the same segment, another three traffic analyzers and cameras were symmetrically positioned (see Fig. 6). Besides, all the data were collected during 8:30 a.m.-11:30 a.m. and/or 14:00 p.m.-17:00 p.m. in no precipitation days, and at least a one-day observation was conducted for every single test to meet the requirement of sample size for structural equations modeling.

4.3.2. Data treatment

(1) Data filtering process

As we focus on a strict car-following situation, so those vehicles in a

Table 1
Variable settings.

Category	Variable	Description
Visual perceptual factor	Temporal frequency (*ft*)	Calculated according to Fig. 1
	Spatial frequency (*fs*)	
Vehicular factor	Leading vehicle type (LVT)	Small vehicle = "1", Large vehicle = "2"
	Following vehicle type (FVT)	
Roadway factor	Radius (R)	R = 1800 m, R = 1200 m, and R = 800 m
	Stopping sight distance (SSD)	Calculated according to formula (1)
	Horizontal sightline offset (HSO)	Calculated according to formula (2)
Crash risk variation indicator	Rate of change of mTTC (r_{mTTC})	Calculated according to formula (5)
	Rate of change of DRAC (r_{DRAC})	Calculated according to formula (6)
Latent variable	Speed risk perception (SRP)	Risk perception originated from speed variations
	Distance risk perception (DRP)	Risk perception originated from distance variations
	Crash risk variation (CRV)	Real-time rear-end crash risk variation of a vehicle while it passes through two observation sections

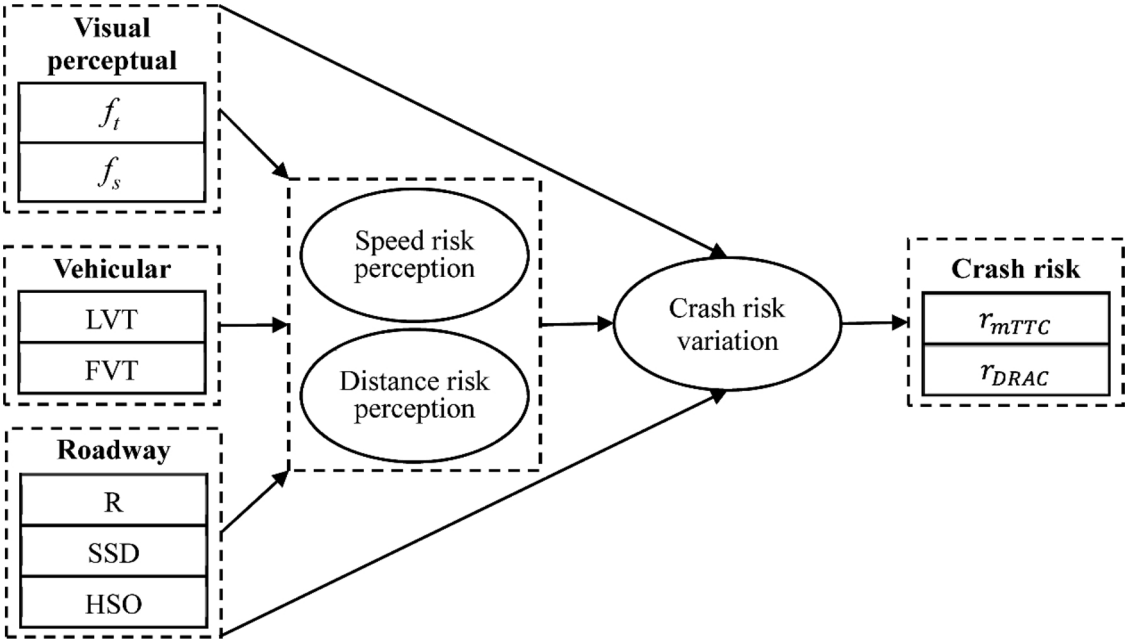

Fig. 3. Theoretical framework for real-time crash risk variation.

Fig. 4. An overview of the segments.

Table 2
Segments profiles.

Segment	KP start (km)	KP end (km)	Radius (m)	Length (m)	Speed limit (km/h)	No. of lanes
Curve1	1251.8	1253.6	1800	477.3	80	4
Curve2	1238.2	1239.3	1200	349.6	80	4
Curve3	1227.3	1228.2	800	404.7	80	4

Note: KP = kilo-post, which indicates the distance measured from the start of the freeway; "Radius" and "Length"are the radius and length of the circular part of the curves; "No. of lanes" is the number of lanes of two-way of the segments in addition to the shoulders.

free-flow state or negotiated lane-change were need to be removed from the sample. Here in this paper, we used the same methods as in our previous study (Ding et al., 2017a) to filter out free-flow and lane-change vehicles. The free-flow vehicles were filtered out by comparing the time headway and the stopping time. That was, if the time headway of a vehicle was greater than its stopping distance, then it was in a free-flow state and need to be removed. Here, the stopping time was calculated as follows $t = V/a$, where t is the stopping time, s; V is the instantaneous speed of a vehicle, m/s; a is the deceleration ($a = 2.5$ m/s^2 was suggested by AASHTO (AASHTO. A policy on geometric design of highways and streets, 2011)). If the state of free-flow and/or lane-change occurred at any section of the three (of one direction of the segment), then the vehicle needed to be removed. To identify the lane-change vehicles, video clips were reviewed frame by frame to check the trajectory of each vehicle from observation section #1 to #3. If lane-change happened between any two consecutive observation sections, then this vehicle needed to be removed from the dataset.

(2) Determine vehicle type

The NC200 traffic analyzers differ the type of vehicles into small, medium, and large ones by detecting vehicle length. For the sake of simplification, and to clearly distinguish the type (size) of vehicles, we chose the small and large vehicles.

(3) Calculation of average temporal frequency

As introduced in Fig. 1, the edge rate (f_t) of vehicle i equals its instantaneous speed v_i divided by λ. Here, considering the impact of the entire 300 m-length line markings, we substituted the instantaneous speed v_i with the average speed of the driving range within the line markings (observation section #1 to #3), so the temporal frequency, that a driver could perceived when it passed through the line markings area, can be calculated as follows:

$$\bar{f}_t = \frac{400}{\lambda \bullet \Delta t} \tag{7}$$

wherein, $\bar{f}_t$ is the average temporal frequency; Δt is the time interval when the vehicle passes through observation section #1 and #3.

(4) Calculation of r_{mTTC} and r_{DRAC}

In this paper, we attempted to compare the effects of different forms of line markings on crash risk variation, so the mTTC and DRAC between observation section #1 and #3 were used to calculate the r_{mTTC} and r_{DRAC}, as follows:

$$r_{mTTC} = \frac{mTTC_i(t_1) - mTTC_i(t_3)}{mTTC_i(t_1)} \tag{8}$$

$$r_{DRAC} = \frac{DRAC_i(t_1) - DRAC_i(t_3)}{DRAC_i(t_1)} \tag{9}$$

where $mTTC_i(t_1)$, $mTTC_i(t_3)$, $DRAC_i(t_1)$, and $DRAC_i(t_3)$ are the mTTC and DRAC of vehicle i as it passed observation section #1 and #3, respectively, and $t_1 < t_3$.

4.4. Data analysis

The Pearson's bivariate correlation analysis was conducted to determine the inter-correlations among observed variables by using R 3.6.0. Confirmatory factor analysis (CFA) was conducted to examine the reliability and validity of the measurement model, and structural equations modeling (SEM) using AMOS 20.0 was employed to examine the hypothesized structural model. Each of the impact coefficients was estimated using the asymptotically distribution-free estimates method. Eight commonly used goodness-of-fit indices were employed to assess the overall model fit. A good fit was indicated by the ratio of χ^2 to degrees of freedom ($\chi^2/df < 3$), the goodness-of-fit index (GFI ≥ 0.90), the adjusted goodness-of-fit index (AGFI ≥ 0.80), the comparative fit index (CFI ≥ 0.90), the normed fit index (NFI ≥ 0.90), the incremental fit index (IFI ≥ 0.90), the Tuckere Lewis index (TLI ≥ 0.90), root mean squareerror of approximation (RMSE < 0.06; RMSEA value as high as 0.08 is considered acceptable).

5. Results

5.1. Descriptive statistics of the sample

The sample consists of 2239 records of individual vehicles. A detailed statistic of the sample and the basic traffic flow data of speed (V), distance headway (DH), and time headway (TH), was show in Table 3. Wherein, there was a total of 1191 small vehicles and 1048 large vehicles. More specifically, there were 612 records of small vehicle following a small vehicle and 579 records of small vehicle following a large one, 528 records of large vehicle following a small vehicle and 520 records of large vehicle following a large one.

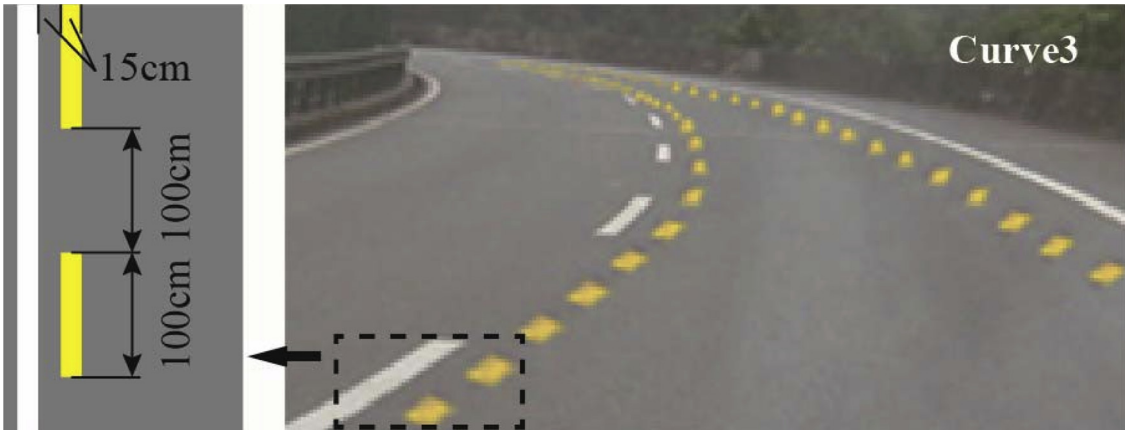

Fig. 5. Design of line markings. Here, the condition of λ = 2 m and R = 800 m was demonstrated as an example.

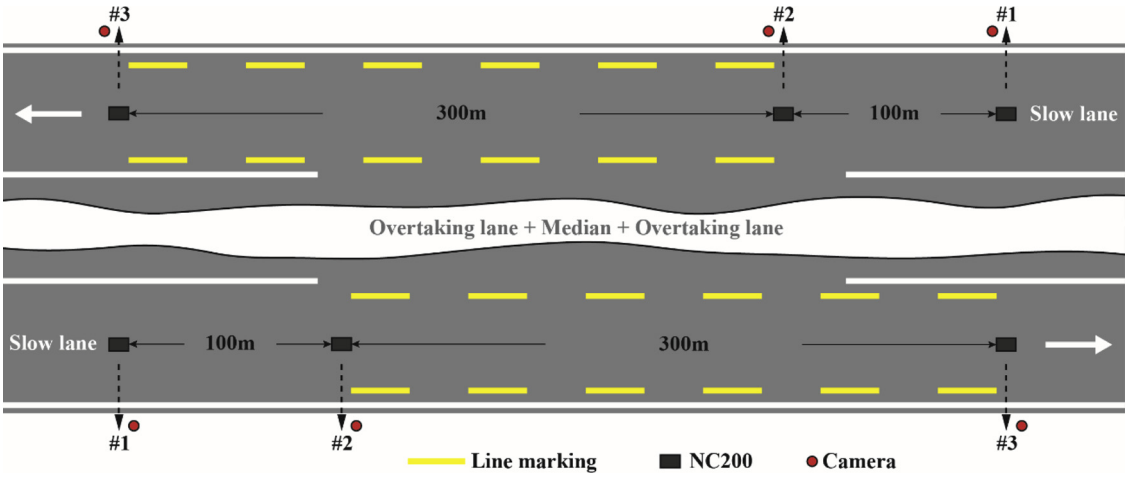

Fig. 6. Layout of traffic analyzers and cameras. Here, the roadway was intentionally depicted as straight for simplification.

5.2. Association among observed variables

Table 4 shows the descriptive characteristics of and correlations among observed variables. In particular, $\bar{f}_t$ correlated significantly and positively with f_s (r = 0.39, p < 0.001), r_{mTTC} (r = 0.15, p < 0.01), and r_{DRAC} (r = 0.13, p < 0.01). Results also indicate that f_s correlated significantly and positively with r_{mTTC} (r = 0.14, p < 0.01), and r_{DRAC} (r = 0.11, p < 0.01). Leading vehicle type (LVT) correlated significantly and positively with r_{mTTC} (r = 0.11, p < 0.05), and r_{DRAC} (r = 0.12, p < 0.05); following vehicle type (FVT) correlated significantly and negatively with r_{mTTC} (r = -0.10, p < 0.05), and r_{DRAC} (r = -0.09, p < 0.05). R had significant correlation with SSD (r = 0.09, p < 0.05), HSO (r = -0.10, p < 0.001), r_{mTTC} (r = 0.13, p < 0.01), and r_{DRAC} (r = 0.11, p < 0.01). SSD had significant correlation with HSO (r = 0.18, p < 0.001), r_{mTTC} (r = 0.13, p < 0.01), and r_{DRAC} (r = 0.12, p < 0.01). HSO had significant correlation with r_{mTTC} (r = 0.10, p < 0.05), and r_{DRAC} (r = 0.11, p < 0.05). The r_{mTTC} significantly correlated with the r_{DRAC} (r = 0.73, p < 0.01). Examination of the correlations revealed that $\bar{f}_t$, f_s, LVT, FVT, R, SSD, and HSO all had relatively strong correlations with the r_{mTTC} and r_{DRAC}.

5.3. Model testing

5.3.1. Measurement model

Although the Chi-square statistic (χ^2 = 30.4, d.f. = 14, p < 0.001) is significant, the measurement model provided reasonable fit to the data according to the goodness-of-fit indices from CFA (see Table 5). In addition, it showed that all the indicators loaded highly (factor loading coefficients > 0.5, p < 0.001) on the appropriate latent variables (i.e., speed risk perception, distance risk perception, and crash risk variation), suggesting that both latent variables under consideration were reliably assessed, and the convergent validity was established.

5.3.2. Structural model

Fig. 7 shows the results of the estimated model, and demonstrates the standardized path coefficients of the significant structural relationships (p < 0.05) among the tested variables. The amount of variance in speed risk perception accounted for by $\bar{f}_t$, f_s, and LVT was 21%. The amount of variance in distance risk perception accounted for by $\bar{f}_t$, f_s, LVT, SSD, HSO, and R was 29%. Speed risk perception and distance risk perception explained 27% of the total variance in crash risk variation. In the model, the crash risk variation was significantly predicted by drivers' speed risk perception (β = 0.49, p < 0.001) and distance risk perception (β = 0.54, p < 0.001). $\bar{f}_t$ (β = 0.81, p < 0.001), f_s (β = 0.47, p < 0.01), and FVT (β = -0.12, p < 0.05) were found to significantly affect drivers' speed risk perception; $\bar{f}_t$ (β = 0.37, p < 0.05), f_s (β = 0.33, p < 0.01), LVT (β = 0.11, p < 0.05), SSD (β = 0.39, p < 0.01), HSO (β = 0.13, p < 0.05), and R (β = -0.10, p < 0.05) were found to significantly affect drivers' distance risk perception. In addition, the r_{mTTC} (β = 0.66, p < 0.001) and r_{DRAC} (β = 0.44, p < 0.01) were found to be confirmative to characterize crash risk variation (CRV).

6. Discussion

In the present study, we examined the role of visual perceptual factors, vehicular factors, and roadway factors in the prediction of real-time crash risk variation by considering speed risk perception and

Table 3
Descriptive statistics of the sample.

Segment	Test	Sample size	Avg. V (m/s)	Std. of V (m/s)	Avg. DH (m)	Std. of DH (m)	Avg. TH (s)	Std. of TH (s)
Curve1	λ = 2m	203	20.9	0.34	94.8	1.07	4.43	0.19
	λ = 4m	187	21.4	0.35	93.2	1.12	4.35	0.14
	λ = 8m	212	21.8	0.33	92.5	1.01	4.13	0.17
	Control	158	22.3	0.34	89.8	1.21	4.08	0.17
Curve2	λ = 2m	214	20.9	0.34	94.7	1.02	4.40	0.15
	λ = 4m	198	21.4	0.33	93.4	0.98	4.32	0.18
	λ = 8m	177	21.7	0.33	92.2	1.06	4.11	0.21
	Control	143	22.2	0.33	89.6	1.16	4.04	0.19
Curve3	λ = 2m	182	20.9	0.34	94.4	1.18	4.36	0.18
	λ = 4m	205	21.3	0.35	92.9	1.15	4.29	0.16
	λ = 8m	209	21.6	0.34	92.2	1.13	4.09	0.20
	Control	151	22.2	0.34	89.5	1.16	4.03	0.21

Note: "Control" means the original roadway condition where no extra line marking was installed.

Table 4
Descriptive characteristics of correlations among observed variables.

Variables	$\bar{f}_t$	f_s	LVT	FVT	R	SSD	HSO	r_{mTTC}	r_{DRAC}
$\bar{f}_t$	1								
f_s	0.39***	1							
LVT	0.01	0.01	1						
FVT	0.02	−0.05	0	1					
R	0.01	0.02	0	0.01	1				
SSD	0.02	0.01	−0.03	0.05	0.09*	1			
HSO	0.01	−0.01	−0.01	−0.03	−0.10***	0.18***	1		
r_{mTTC}	0.15**	0.14**	0.11**	−0.10*	0.13**	0.13**	0.10*	1	
r_{DRAC}	0.13**	0.11**	0.12**	−0.09*	0.11**	0.12**	0.11*	0.73**	1

* $p < 0.05$, ** $p < 0.01$, *** $p < 0.001$.

Table 5
Fit indices for the tested model.

Fit indices	Recommended value	Tested model
χ2/d.f.	1-3	2.17
GFI	≥0.9	1.00
AGFI	≥0.8	1.00
CFI	≥0.9	0.97
NFI	≥0.9	0.94
IFI	≥0.9	0.96
TLI	≥0.9	0.92
RMESA	≤0.08	0.05

distance risk perception within an integrated structural equations model. Results from the SEM demonstrated that the data fit well with our theoretical model with significant paths showed the predictive power of driver's visual perceptual parameters (i.e., f_t and f_s), vehicle size (i.e., LVT and FVT), and roadway alignment parameters (i.e., radius, SSD, and HSO) on real-time crash risk variation (reduction) under the influence of line markings.

In general, the contribution of the present work to the literature is three-folded: (1) we incorporated driver's visual perception into the form of crash risk and its variation, and quantitatively determined the causal relationship between visual perceptual factors and crash risk variation by introducing the optical flow parameters of f_t and f_s. This could be deemed as an extension and advance to the previous research endeavors regarding human factors as a predictor in the link between driver's visual perception and driving outcomes (Liu et al., 2013; Rakha et al., 2006; Ding et al., 2017a; Ding et al., 2017b; Ding et al., 2019). Also, our findings, to certain extent, is a practical usage of theories in visual perception (Gibson, 1950; Sinai et al., 1998; Yarbrough et al., 2002; Wu et al., 2004; Feria et al., 2003) to the driving scenario. (2) our findings preliminarily differentiated driver's risk perception from speed and distance, i.e., the speed risk perception and distance risk perception, and clarified the contributions of these two original sources of risk perception on crash risk variation during a short time or distance. (3) unlike previous research that measured crash risk directly by those surrogate safety indicators, such as TTC and/or DRAC (Abdel-Aty et al., 2005; Xu et al., 2013; Li et al., 2014;Li et al., 2017; Mahmud et al., 2017), we extended and modified the indicators into the rate of change of the indicators, to attempt to match the crash risk variation during a short time interval or distance range.

In particular, our study found a high percentage of explained variance (27%) in crash risk variation that associated with visual perceptual, vehicular, and roadway factors. This value was higher than the results of the similar studies of Mallia et al. (2015) and Tao et al. (2017), which were commonly limited to 10%. One obvious reason for this could be that we focused on the crash risk variation caused by the installed line markings while the previous studies emphasized on the crash risk per se that induced directly by risky driving behavior (Mallia et al., 2015) and/or personality traits Tao et al. (2017). Another plausible reason could be that we introduced two extended and modified proximal indicators to measure the aforementioned variation of crash risk. Besides, unlike previous studies that based on socio-demographic investigation or questionnaire, we resort to field observation to collect naturalistic driving data to expect to characterize the real driving

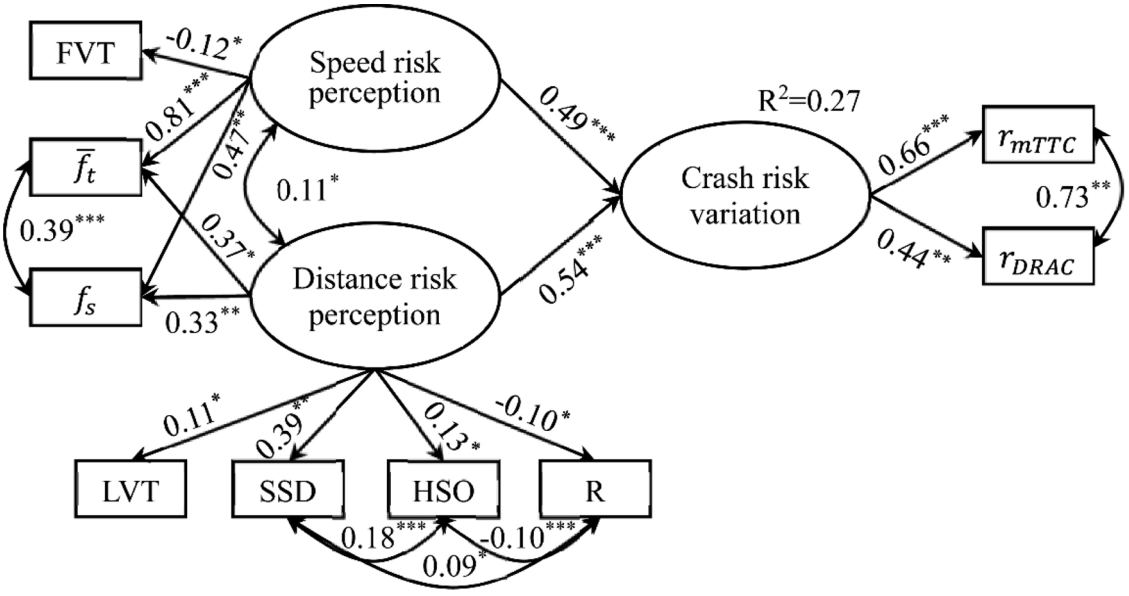

Fig. 7. The final SEM and standardized path coefficients. *p < 0.05; **p < 0.01; ***p < 0.001.

behaviors.

In addition, our findings also provided new insights on the factors contributive to crash risk. And the influence of the visual perceptual, vehicular, and roadway factors on crash risk variation that demonstrated in our SEM could be detailed as follows, respectively.

6.1. Effects of line markings

As reviewed in the introduction, explanations for the effects of line markings on crash risk variation could be three-folded. First, drivers' perception of distance could be affected by the "discontinuity effect" (Feria et al., 2003) produced by the discontinuous line markings. Similar to the textures in the experiments of Sinai et al. (1998), Yarbrough et al. (2002), (Wu et al. (2004), and Feria et al. (2003), to certain extents, the line markings in the present study could be regarded as discontinuous textures on road surface. Accordingly, the distance to the leading vehicle could be underestimated by the following drivers. However, for safety, drivers inclined to (or had to) increase its following headway to compromise the crash risk. Second, drivers' perception of speed could be affected by the edge rate information produced by the line markings. According to Rakha et al. (2006), Francois et al. (2011), Liu et al. (2013), and Ding et al. (2017a), Ding et al. (2017b), Ding et al. (2019) edge rate could induce speed overestimations of drivers, which eventually gave rise to the reduction in its actual speeds. In the present study, the drivers may experience with edge rate as there was relative motion between the line markings and the drivers while the vehicle passed through. And the edge rate could lead to speed reduction. So, since the drivers' risk perceptions of speed and distance were changed, the entire crash risk was then fluctuated. And to be specific, the crash risk was reduced. Furthermore, a high density of the discontinuous line markings may lead to a greater "discontinuity effect", since a severer disruption was acted on the original continuous road surface in condition of $\lambda = 2$ m. Besides, Liu et al. (2013) found that when the value of edge rate fell in [8 Hz, 16 Hz], drivers could be most visually sensitive to the edge rate, which resulted in the greatest effect of speed reduction. Besides, one of our previous study found a similar interval of the value of edge rate ([5 Hz, 14 Hz]), in which the time headway increased as the edge rate increased Ding et al. (2017a). These results could be evidences for explaining the positive relationship between $\bar{f}_t$ (or f_s) and r_{mTTC} (or r_{DRAC}).

6.2. Effects of vehicle type

According to the SEM, the following vehicle type (FVT) was negatively related with speed risk perception (SRP). This could be attributed to two reasons that concerning the different car-following behaviors of different types of vehicles (Peeta et al., 2005). First, apparently, the speed of large vehicles is usually lower than the speed of the small ones. That means a truck driver would perceive a smaller edge rate than the car driver even though they see the same line markings on roadway. Accordingly, there would be smaller variation of crash risk among the trucks than that of the cars. Second, in a perspective of visual perception, the speed of an observer would perceive is greatly optically determined (Gibson, 1950; Fajen, 2008), which can be characterized by optical flow rate created by (Gibson, 1950). Optical flow rate, an optical variable similar with edge rate, is proportional to speed and inversely proportional to the observers' eye height above the surface it stands. So, in our experiment, a truck driver would be less effectively affected by the line markings regarding the speed reduction and its corresponding result of crash risk variation, since the eye height of a truck driver is significantly greater than that of a car driver with respect to the roadway.

The effects of leading vehicle type (LVT) could be derived from the size perception of drivers. More specifically, it related to the visual angle between the following driver and its leading vehicle. This visual angle is an important basis for the following drivers to estimate the relative distance. In the car-following situation, this angle changes as the relative distance changes. According to the geometric relationship depicted in Fig. 8, the visual angle can be calculated as follows.

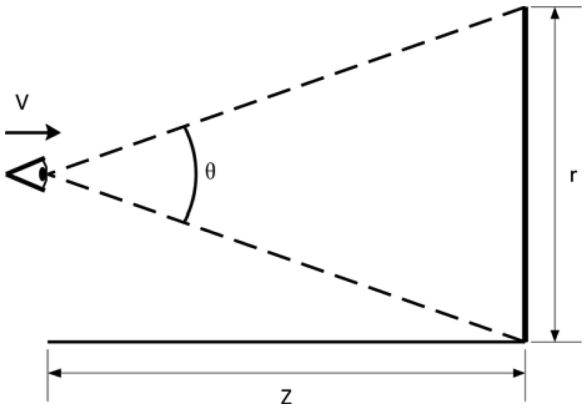

Fig. 8. A sketch of geographic relationship between drives' visual angle and distance.

$$\theta = 2\tan^{-1}(r/z),\ z = r/\tan(\theta/2) \tag{10}$$

where, θ is the visual angle between the eye and the leading vehicle; z is the distance between the following and the leading vehicle, m; r is the height of the leading vehicle, m.

Deriving the above equations with time, we can get:

$$v = -kr/2\sin^2(\theta/2),\ v = (k^2t/2)\csc^2(\theta/2)\cot(\theta/2) \tag{11}$$

where, v is the speed of the leading vehicle, m/s; k is the deceleration of the following vehicle, m/s^2。

According to Lee's τ theory (Lee, 1976), there was a relationship among the visual angle, distance, and speed, and that was:

$$\tau = \theta/\theta^{'} = z/v,\ \tau^{'} = -1 + (zk/v^2) \tag{12}$$

Then, bring formula (11) into formula (12), we can get:

$$\tau = (-2/k)\sin(\theta/2)\cos(\theta/2),\ \tau^{'} = -1 + 2\cos^2\cos(\theta/2) \tag{13}$$

From the formulas above, it can be discovered that, under the situation of an equivalent speed and distance, a large vehicle would lead to a relative small value of $\tau^{'}$ since the visual angle θ was big. Furthermore, according to the studies of Yilmaz and Warren (1995) and Andersen et al. (1999), the drivers would increase its braking force to avoid a possible crash, which generated a greater deceleration, when the value of $\tau^{'}$ was small. Therefore, when there was large vehicle ahead, the following drivers would decelerate with a greater deceleration to compromise the crash risk, which eventually gave rise to the reduction in crash risk.

6.3. Effects of curves

According to the SEM, the radius was negatively and the SSD and HSO were positively related with crash risk variation when explained from the perspective of distance risk perception of drivers. This could be separately explained by SSD and R.

As stated by Fambro et al. (1997), Wood and Donnell (2014), Wood and Donnell (2017), Retting et al. (2000), and Gargoum et al. (2018), SSD and HSO are critical for a driver to successfully avoid a pending crash especially on curves. Indeed, it is not just a determinative parameter that should be carefully designed, it is more of a standard of mental and physical requirement of the drivers while negotiating on curves. More accurately, according to the Green Book (AASHTO. A policy on geometric design of highways and streets, 2011), SSD is a function of design speed, driver perception-reaction times, and driver deceleration rates, and HSO is associated with SSD and R (radius of the curve), as shown in formula (1) and (2). So, it can be discovered that a

driver in a relatively high speed would require a greater SSD and HSO for successful crash avoidance than its counterparts in low speed. It means that at drivers on curves with large radius or at high speed would be more likely to perceive the risk derived from distance changes, which leads to a relative greater variation in crash risk.

On the other hand, the effect of curves could be interpreted by radius (R) independently. The effect of radius of the curved segment is consistent with the previous studies of Ni and Andersen (2008) and Bian et al. (2013), which argued that the following drivers utilized the rate of bearing change of the leading vehicle while negotiating on curves. And they held that drivers were less sensitive in detecting a crash on a curve with a small radius than a curve with a large radius, due to a greater rate of bearing change on the small radius curve. In addition, Ni and Andersen (2008) believed that, aside from the rate of bearing change, more information were needed for drivers to successfully avoid a crash when they drove on a curved trajectory with a small radius. It means that, on curves with small radius, there was relatively less chance for drivers to properly adjust its driving behaviors to compensate any perceived crash risk, which resulted in fewer variation in crash risk. Besides, Zhang et al. (2013) had another explanation on this effect. He argued that drivers would predominately rely on the second-order motion information (i.e., deceleration) to judge the curvature magnitude of a curved segment and to recover depth for crash avoidance. However, they were not as sensitive to the second-order motion information as they were with the first-order motion information (i.e., speed). So, this deficiency might aggravate the fact that the drivers were less likely to perceive the crash risk while following a vehicle on a curve with a small radius.

6.4. General effects of SRP and DRP

As shown in the Fig. 7, the standardized effect of distance risk perception (0.54) on crash risk variation (CRV) was slightly greater than that of speed risk perception (0.49). It means the drivers' distance risk perception could lead to a greater change in crash risk variation than the speed risk perception. On the one hand, this could be that the distance risk perception was measured by more variables (f_t, f_s, LVT, SSD, HSO, and R) than the speed risk perception (f_t, f_s, and FVT), which might result in a relatively more comprehensive interpretation and explanatory of the distance risk perception on crash risk variation. On the other hand, this difference may be mentally inherent in drivers' risk perception. That is, the changes in distance to the leading vehicle could be the direct visual stimulus of risk, while the changes in speed would be an indirect one comparatively. Apparently, distance is a fundamental spatial information, like the shape, size, and position of an object, in the first place that we can "read" directly or can be measured in depth directly (as suggested by Gibson (1950)); yet speed is a motion information, which is based on the three-dimensional space, that need more computational efforts in mental of us before it could be accurately understood (Baker, 1999). And this difference could be easily discovered in the unit of these two variables, that is, distance is measured by meter (m) while speed is measured by meter per second (m/s) in System International (SI). Actually, this difference could make substantial sense as for driving situation. On highways, even though in a high speed, a driver may not need to pay too much attention to its speed and the crash risk, when there is no vehicle ahead in its visual field; but the driver has to be cautious to avoid a crash when he is closely following a vehicle, even if he drives slowly. As the crash risk could be predicted by the change in distance more directly, so the drivers' distance risk perception generated in a relatively greater impact on the crash risk variation.

7. Conclusion

Overall, in this study, we attempted to explain drivers' crash risk variation in car-following for crash avoidance considering the effects of drivers' visual perception, vehicle type, and horizontal curves, by installing a series of line markings on the curve segments of a freeway in China. A structural equations model was built to associate the crash risk variation with these factors by incorporating drivers' speed risk perception and distance risk perception as latent variables. The results from the structural equations model indicate that (1) the amount of variance in speed risk perception accounted for by $\bar{f}_t$, f_s, and FVT was 21%; (2) the amount of variance in distance risk perception accounted for by $\bar{f}_t$, f_s, LVT, SSD, HSO, and R was 29%; (3) speed risk perception and distance risk perception explained 27% of the total variance in crash risk variation. The results were explained from the perspective of the effect of line markings, vehicle type (size), and curves on driving behaviors, respectively. In addition, the difference between the effect of speed risk perception and distance perception on crash risk variation was preliminarily discussed considering the direct and indirect origins of risk in driving.

However, there are limitations in that, (1) we believe the visual perceptual factors and the roadway factors may have direct impact on crash risk variation, but in this study, we failed to find out any evidence to support it; (2) visual perception is a relatively broad concept in psychology, so there might be the concern that if the drivers' visual perception can be adequately characterized by temporal frequency (f_t) and/or spatial frequency (f_s), and indeed there are many other visual cues, i.e., texture gradient, linear perspective, for recovering speed and distance; (3) the personal traits, like gender, age, etc., might also be influential to car-following behaviors and its subsequent crash risk variation. These issues and/or factors were intentionally ignored in the present study for the sake of simplification and clarity, but are within considerations of our future research.

Declaration of Competing Interest

The authors declare that they have no known competing financial interests or personal relationships that could have appeared to influence the work reported in this paper.

Acknowledgements

This work was supported by the National Natural Science Foundation of China (grant number 71901166, 71801176, 71771183); the Science and Technology Project of Department of Transportation of Hubei Province (grant number 2018-422-3-4); the Research Project of Hubei Provincial Department of Education(grant number Q21091509); and the Scientific Research Foundation of Wuhan Institute of Technology (grant number K201845).

References

WHO, 2018. Global Status Report on Road Safety 2018. World Health Organization (WHO), Geneva.
Traffic Management Bureau of the Public Security Ministry, 2018. Annual statistics of road traffic accidents of People's Republic of China (2017). Traffic Management Bureau of the Public Security Ministry, People's Republic of China, Beijing in Chinese.
AASHTO, 2010. Highway Safety Manual (2010). American Association of State Highway and Transportation Officials (AASHTO), Washington D.C.
Dewar, R.E., Olson, P.L., 2007. Human Factors in Traffic Safety, 2nd edition. Tucson: Lawyers & Judges Publishing Company.
Sivak, M., 1996. The information that drivers use: is it indeed 90% visual? Perception 25 (9), 1081–1089.
Golob, T.F., Recker, W.W., Alvarez, V.M., 2004. Freeway safety as a function of traffic flow. Accid. Anal. Prev. 36 (6), 933–946.
Nagatani, T., 2015. Effect of vehicular size on chain-reaction crash. Phys. A Stat. Mech. Appl. 438, 132–139.
Harwood, D.W., Bauer, K.M., 2015. Effect of stopping sight distance on crashes at crest vertical curves on rural two-lane highways. Transp. Res. Rec. 2486, 45–53.
Wood, J.S., Donnell, E.T., 2014. Stopping sight distance and horizontal sight line offsets at horizontal curves. Transp. Res. Rec. 2436, 43–50.
Wood, J.S., Donnell, E.T., 2017. Stopping sight distance and available sight distance new model and reliability analysis comparison. Transp. Res. Rec. 2638, 1–9.
Gibson, J.J., 1950. The Perception of the Visual World. Houghton Mifflin, Boston.
Warren, R., 1982. Optical Transformations During Movement: Review of the Optical

Concomitants of Egospeed. Ohio State University, Department of Psychology, Aviation Psychology Laboratory, Columbus.
Drakopoulos, A., Vergou, G., 2003. Evaluation of the Converging Chevron Pavement Marking Pattern at One Wisconsin Location. AAA Foundation for Traffic Safety, Washington, DC.
Gates, T.J., Qin, X., Noyce, D.A., 2008. Effectiveness of experimental transverse-bar pavement marking as speed-reduction treatment on freeway curves. Transp. Res. Rec. 2056, 95–103.
Martindale, A., Urlich, C., 2010. Effectiveness of Transverse Road Markings on Reducing Vehicle Speeds. Wellington, NZ Transport Agency.
Liu, B., Zhu, S.Y., Wang, H., et al., 2013. Optimization design and experiment on plane layout of edge line marking for speed reduction. TRB 92nd Annual Meeting Compendium of Papers 13–3528.
Zhao, X., Ding, H., Lin, Z., et al., 2018. Effects of longitudinal speed reduction markings on left-turn direct connectors. Accid. Anal. Prev. 115, 41–52.
Denton, G.G., 1980. The influence of visual pattern on perceived speed. Perception 9 (4), 393–402.
Retting, R.A., Mcgee, H.W., Farmer, C.M., 2000. Influence of experimental pavement markings on urban freeway exit-ramp traffic speeds. Transp. Res. Rec. 1705, 116–121.
Rakha, H.A., Katz, B.J., Duke, D., 2006. Design and evaluation of peripheral transverse bars to reduce vehicle speed. TRB 85th Annual Meeting Compendium of Papers 06–0577.
Francois, M., Morice, A.H., Bootsma, R.J., et al., 2011. Visual control of walking velocity. Neurosci. Res. 70 (2), 214–219.
Godley, S.T., Triggs, T.J., Fildes, B.N., 2000. Speed reduction mechanisms of transverse lines. Transp. Hum. Factors 2 (4), 297–312.
Sinai, M.J., Ooi, T.L., He, Z.J., 1998. Terrain influences the accurate judgment of distance. Nature 395, 497–500.
Yarbrough, G.L., Wu, B., Wu, J., Ooi, T.L., 2002. Judgments of object location behind an obstacle depend on the particular information selected. J. Vis. 2 (7) 625-625.
Wu, B., Ooi, T.L., He, Z.J., 2004. Perceiving distance accurately by a directional process of integrating ground information. Nature 428, 73–77.
Feria, C.S., Braunstein, M.L., Andersen, G.J., 2003. Judging distance across texture discontinuities. Perception 32 (12), 1423–1440.
Ding, N., Zhu, S., Wang, H., et al., 2017a. Effects of edge rate of designed line markings on following time headway. Sci. Iran. 24 (4), 1770–1778.
Ding, N., Zhu, S., Wang, H., et al., 2017b. Following safely on curved segments: a measure with discontinuous line markings to increase the time headways. Iran. J. Sci. Technol. Trans. Civ. Eng. 41 (3), 351–359.
Ding, N., Zhu, S., Wang, H., et al., 2019. Effects of reverse linear perspective of transverse line markings on car-following headway: a naturalistic driving study. Saf. Sci. 119C, 50–57. https://doi.org/10.1016/j.ssci.2018.08.021. in press.
Peeta, S., Zhang, P., Zhou, W., 2005. Behavior-based analysis of freeway car-truck interactions and related mitigation strategies. Transp. Res. Part B Methodol. 39 (5), 417–451.
Yoo, H., Green, P., 1999. Driver Behavior While Following Cars, Trucks, and Buses. The University of Michigan Transportation Research Institute.
Jiang, J., Lu, J., Lv, Z., 2011. Car-following behavior of different vehicles on ordinary highways. Proceedings of International Conference of Chinese Transportation Professionals 1822–1831.
Yilmaz, E.H., Warren, W.H., 1995. Visual control of braking: a test of the tau hypothesis. J. Exp. Psychol. Hum. Percept. Perform. 21 (5), 996–1014.
Andersen, G.J., Cisneros, J., Atchley, P., et al., 1999. Speed, size, and edge-rate information for the detection of crash events. J. Exp. Psychol. Hum. Percept. Perform. 25 (1), 256–269.
Lee, D.N., 1976. A theory of visual control of braking based on information about time-to-crash. Perception 5 (4), 437–459.
Zegeer, C., Stewart, R., Reinfurt, D., 1991. Cost-effective Geometric Improvements for Safety Upgrading of Horizontal Curves. Report FHWA-RD-90-021. FHWA, U.S. Department of Transportation.
Schneider, W.H., Zimmerman, K., Van Boxel, D., et al., 2009. Bayesian analysis of the effect of horizontal curvature on truck crashes using training and validation data sets. Transp. Res. Rec. 2096, 41–46.
Schneider IV, W.H., Savolainen, P.T., Moore, D.N., 2010. Effects of horizontal curvature on single- vehicle motorcycle crashes along rural two-lane highways. Transp. Res. Rec. 2194, 91–98.
Khan, G., Bill, A.R., Chitturi, M., et al., 2012. Horizontal curves, signs, and safety. Transp. Res. Rec. 2279, 124–131.
Ni, R., Andersen, G.J., 2008. Detection of crash events on curved trajectories: optical information from invariant rate-of-bearing change. Percept. Psychophys. 70 (7), 1314–1324.
Zhang, J., Braunstein, M.L., Andersen, G.J., 2013. Effects of changes in size, speed, and distance on the perception of curved 3-d trajectories. Atten. Percept. Psychophys. 75 (1), 68–82.
Bian, Z., Guindon, A.H., Andersen, G.J., 2013. Aging and detection of crash events on curved trajectories. Accid. Anal. Prev. 50 (1), 926–933.
Llopis-Castelló, D., Findley, D.J., Camacho-Torregrosa, F.J., et al., 2019. Calibration of inertial consistency models on North Carolina two-lane rural roads. Accid. Anal. Prev. 127, 236–245.
Fambro, D.B., Fitzpatrick, K., Koppa, R.J., 1997. NCHRP Report 400: Determination of Stopping Sight Distances. TRB. National Research Council, Washington, D.C.
AASHTO. A Policy on Geometric Design of Highways and Streets, 2011. American Association of State Highway Transportation Officials (AASHTO), Washington, D.C. 2011. .
Himes, S.C., Donnell, E.T., 2014. Reliability approach to horizontal curve design. Transp. Res. Rec. 2436, 51–59.
Gargoum, S.A., Tawfeek, M.H., El-Basyouny, K., et al., 2018. Available sight distance on existing highways: meeting stopping sight distance requirements of an aging population. Accid. Anal. Prev. 112, 56–68.
Abdel-Aty, M., Uddin, N., Pande, A., 2005. Split models for predicting multivehicle crashes during high-speed and low-speed operating conditions on freeways. Transp. Res. Rec. 1908, 51–58.
Xu, C., Liu, P., Wang, W., 2013. Development of a crash risk index to identify real time crash risks on freeways. KSCE J. Civ. Eng. 17 (7), 1788–1797.
Li, Z., Ahn, S., Chung, K., 2014. Surrogate safety measure for evaluating rear-end crash risk related to kinematic waves near freeway recurrent bottlenecks. Accid. Anal. Prev. 64, 52–61.
Li, Y., Wang, H., Wang, W., 2017. Evaluation of the impacts of cooperative adaptive cruise control on reducing rear-end crash risks on freeways. Accid. Anal. Prev. 98, 87–95.
Mahmud, S.M.S., Ferreira, L., Hoque, M., 2017. Application of proximal surrogate indicators for safety evaluation: a review of recent developments and research needs. IATSS Res. 41, 153–163.
Washington, S.P., Karlaftis, M.G., Mannering, F.L., 2010. Statistical and Econometric Methods for Transportation Data Analysis. CRC Press.
Mallia, L., Lazuras, L., Violani, C., et al., 2015. Crash risk and aberrant driving behaviors among bus drivers: the role of personality and attitudes towards traffic safety. Accid. Anal. Prev. 79, 145–151.
Tao, D., Zhang, R., Qu, X., 2017. The role of personality traits and driving experience in self-reported risky driving behaviors and accident risk among Chinese drivers. Accid. Anal. Prev. 99, 228–235.
Fajen, B.R., 2008. Perceptual learning and the visual control of braking. Percept. Psychophys. 70 (6), 1117–1129.
Baker, R.G.V., 1999. On the quantum mechanics of optic flow and its application to driving in uncertain environments. Transp. Res. Part F Traffic Psychol. Behav. 2, 27–53.